GEOLOGY | THE GEOLOGICAL SOCIETY OF AMERICA®

https://doi.org/10.1130/G49492.1

Manuscript received 14 July 2021
Revised manuscript received 6 September 2021
Manuscript accepted 2 October 2021

Published online 03 December 2021



# Could the Réunion plume have thinned the Indian craton?

Jyotirmoy Paul* and Attreyee Ghosh
Centre for Earth Sciences, Indian Institute of Science, Bangalore 560012, India

## ABSTRACT

**Thick and highly viscous roots are the key to cratonic survival. Nevertheless, cratonic roots can be destroyed under certain geological scenarios. Eruption of mantle plumes underneath cratons can reduce root viscosity and thus make them more prone to deformation by mantle convection. It has been proposed that the Indian craton could have been thinned due to eruption of the Réunion plume underneath it at ca. 65 Ma. In this study, we constructed spherical time-dependent forward mantle convection models to investigate whether the Réunion plume eruption could have reduced the Indian craton thickness. Along with testing the effect of different strengths of craton and its surrounding asthenosphere, we examined the effect of temperature-dependent viscosity on craton deformation. Our results show that the plume-induced thermomechanical erosion could have reduced the Indian craton thickness by as much as ~130 km in the presence of temperature-dependent viscosity. We also find that the plume material could have lubricated the lithosphere-asthenosphere boundary region beneath the Indian plate. This could be a potential reason for acceleration of the Indian plate since 65 Ma.**

## INTRODUCTION

Cratonic lithosphere commonly reaches a thickness of 250–300 km, which is more than twice the thickness of the average lithosphere (~100 km) (e.g., Conrad and Lithgow-Bertelloni, 2006). Thick and highly viscous roots are the primary reasons for the survival of cratons over billions of years (Lenardic et al., 2003; Paul and Ghosh, 2020). However, some cratons have been reported to have been completely destroyed (e.g., North China craton; Wang et al., 2016) or partially destroyed (e.g., Tanzania craton; Wang et al., 2016) depending on various geological conditions (Lee et al., 2011) and shape (Cooper et al., 2020). Newer studies have suggested that formation of a weak mid-lithospheric discontinuity could also be a potential reason for craton destruction (Kovács et al., 2021). The thickness of the Indian craton has so far remained controversial. Using teleseismic P-wave arrivals, Srinagesh et al. (1989) showed the South Indian craton to be ~300 km thick. Artemieva (2006) estimated the thermal thickness of the Indian craton to be ~230 km. A magnetotelluric study found the Indian craton thickness to be at least 200 km (Naganjaneyulu and Santosh, 2012). Using pressure-temperature calculations from kimberlite xenoliths, Ganguly and Bhattacharya (1987) estimated that the South Indian craton was >185 km thick during the mid-Proterozoic. Maurya et al. (2016) estimated various thicknesses of the Indian craton ranging from 120 km to 250 km, from their surface-wave inversion study. In contrast to those studies, Pandey and Agrawal (1999) studied the thermal structure of the Indian craton and found the average thickness to be restricted to ~104 km, which is quite thin compared to the global average craton thickness. Conrad and Lithgow-Bertelloni (2006), in their global model, also found a very thin craton thickness of ~100 km under the Indian plate. Koptev and Ershov (2011) estimated the thermal thickness of the Indian craton to be ~80–120 km. Another P-wave receiver function study found that the eastern Indian craton thickness is restricted to 78–81 km (Mandal, 2017). Kumar et al. (2007) used a receiver function to showed that the Indian craton thickness barely exceeds 100 km. Recent studies by Singh et al. (2021) also argued for a thinner Indian craton. One possible explanation for a thinner Indian cratonic lithosphere is its interaction with several mantle plumes (Kumar et al., 2007; Cande and Stegman, 2011; van Hinsbergen et al., 2011) as it was splitting from Gondwanaland (Fig. 1).

Mantle plumes can weaken the base of the lithosphere, which could be mechanically eroded by the convective stresses exerted by mantle flow (Davies, 1994). We tested this hypothesis on the Indian craton to evaluate the effect of eruption of the Réunion plume on the craton thickness. We examined several models of different craton and asthenosphere viscosities. We also incorporated temperature-dependent viscosity to analyze the effect of plume-induced weakening on craton thinning, and discuss its implication on the higher velocity of the Indian plate since 65 Ma.

## CONVECTION MODELING

We developed time-dependent forward mantle convection models from 65 Ma to the present day using CitcomS software (Zhong et al., 2000; https://geodynamics.org/cig/software/citcoms/). Outputs were generated at ~1° × 1° horizontal resolution and ~24 km vertical resolution to 300 km depth. The present-day craton locations were obtained from Nataf and Ricard (1996), and then reconstructed back to 65 Ma using the Matthews et al. (2016) reconstruction model in GPlates software (Boyden et al., 2011; https://www.gplates.org). We used reconstructed plate velocities at 1 m.y. intervals to drive mantle convection from 65 Ma to the present day. The Rayleigh number, thermal diffusivity, thermal expansion coefficient, and reference viscosity were $4 \times 10^8$, $10^{-6}$ m$^2$/s, $3 \times 10^{-5}$ K$^{-1}$, and $10^{21}$ Pa·s, respectively. We inserted a mantle plume with a temperature of 1600 °C (800 °C hotter than the ambient mantle) at the location of the Réunion hotspot (55°E, 20°S) (Figs. 1 and 2). Because it is impossible to know the exact shape of the plume at 65 Ma, we constructed the geometry of the plume based on the general idea that a plume has a thick head (Campbell, 2005), a broad tail, and a pinched intermediate part (French and Romanowicz, 2015). In our models, the plume has a thick head of ~1000 km diameter to 600 km depth, followed by a narrow tail having a radius of ~600 km between 600 and 2000 km depth, and a broad base of ~1000 km diameter from 2000 km depth to the core-mantle boundary (Fig. 2A).

We divided the mantle into four different rheological layers (lithosphere, 0–100 km; asthenosphere, 100–300 km; upper mantle, 300–660 km; lower mantle, 660–2900 km) of different relative viscosities normalized against the reference viscosity of $10^{21}$ Pa·s. Viscosity of

*E-mail: jyotirmoyp@iisc.ac.in

CITATION: Paul, J., and Ghosh, A., 2021, Could the Réunion plume have thinned the Indian craton?: Geology, v. XX, p. , https://doi.org/10.1130/G49492.1

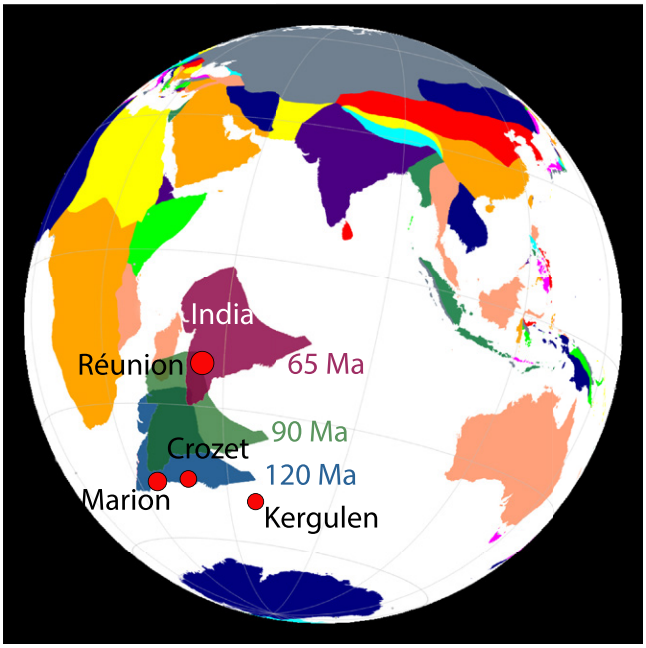


**Figure 1. Map showing location of the Indian plate at different times using the plate reconstruction model of Matthews et al. (2016). The location of the Indian lithosphere at 65 Ma, 90 Ma, and 120 Ma is shown in magenta, green, and blue, respectively; present-day location is shown in purple. Red circles indicate locations of four labeled hotspots. Present-day locations of other smaller plates are shown in different colors.**

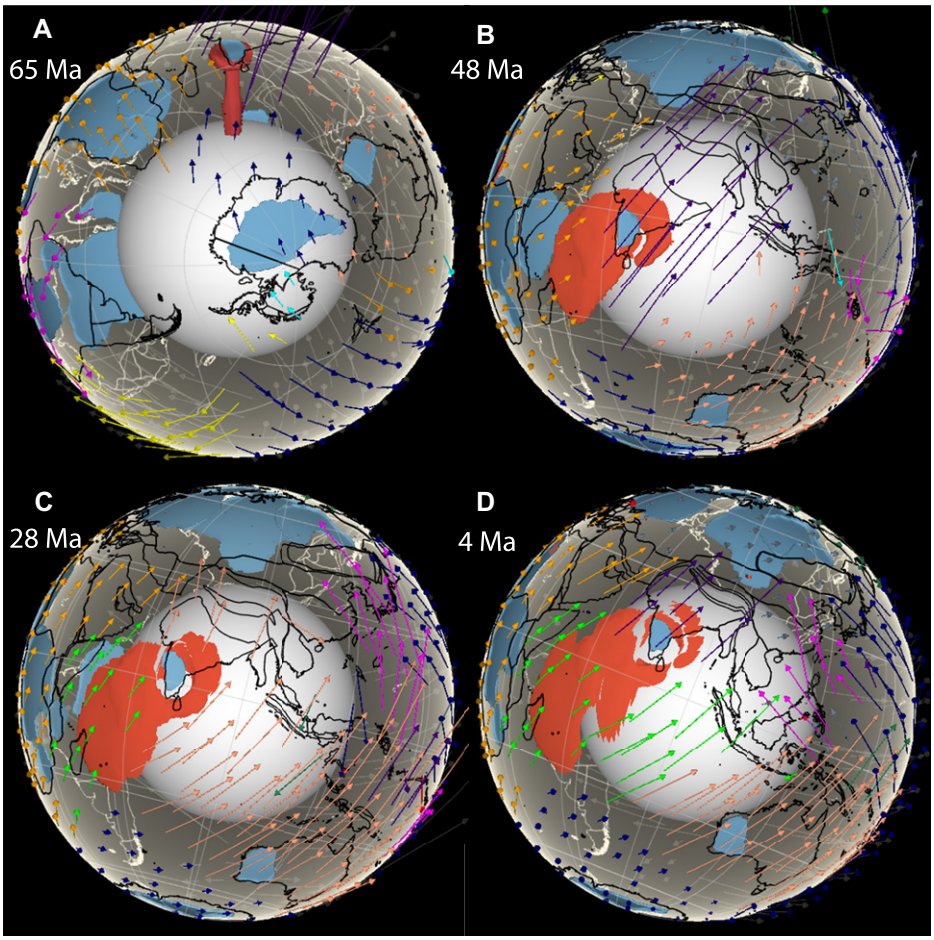


**Figure 2. Viscosity isosurface maps showing the evolution of the Indian craton in the presence of the Réunion plume from the model with asthenosphere and craton viscosity (relative to the reference viscosity of $10^{21}$ Pa·s) combination of (1, 100) and $E = 10$ (where $E$ indicates strength of temperature dependence of viscosity; see text). Réunion plume is marked by red color, and cratons are marked by blue. Respective times are listed in each panel. With time, plume material is dragged along the Indian plate and might have formed a lubricated lithosphere-asthenosphere boundary underneath the plate. Arrows indicate reconstructed plate velocities. Colored arrows represent velocities of different plates. The surface of the white sphere indicates the core-mantle boundary. Black and white borders indicate coastline.**

the lithosphere was kept constant at $30 \times 10^{21}$ Pa·s; viscosity of the asthenosphere was varied between $10^{20}$ and $10^{21}$ Pa·s (relative viscosity of 0.1–1). Upper-mantle viscosity was same as the reference viscosity of $10^{21}$ Pa·s, and the lower mantle was 50× more viscous than the upper mantle. Cratons were made 100× to 1000× more viscous than their surroundings, and initially were 300 km thick. With these viscosity combinations, we created four primary models: (0.1, 100), (0.1, 1000), (1, 100), and (1, 1000), where the two numbers within each pair of parentheses denote the relative viscosity of the asthenosphere and of the craton, respectively. We neglected other weaker viscosity combinations because our previous studies showed that they are unable to support the craton's long-term stability (Paul et al., 2019; Paul and Ghosh, 2020). In our models, cratons are characterized by their high viscosity, i.e., $>30 \times 10^{21}$ Pa·s in the top 100 km, and $>10^{21}$ and $>10^{22}$ Pa·s at 100–300 km depth when asthenosphere viscosities are $10^{20}$ and $10^{21}$ Pa·s, respectively.

We calculated temperature-dependent viscosity ($\eta$) according to the linearized Arrhenius law, $\eta = \eta_o \times \exp[E(T_o - T)]$, where $\eta_o$ is the ambient layer viscosity, $T$ and $T_o$ are the non-dimensionalized actual and reference temperatures, respectively, and $E$ indicates the strength of temperature dependence. With increasing values of $E$, higher-temperature anomalies produce low-viscosity regions, and vice versa. We tested three different $E$ values of 0, 5, and 10, which translate to 1×, 10×, and 100× of viscosity variation compared to the reference viscosity, to examine the effect of temperature-dependent viscosity on Indian craton dynamics. There are four scenarios for each relative viscosity combination model. First, we investigated the evolution of the Indian craton in the absence of a plume. Next, we included a plume but kept $E = 0$. Subsequently, we increased the values of $E$ to 5 and 10. From these models, we infer the nature of the evolution of the Indian craton.

## PLUME-CRATON INTERACTION

The Indian craton self-consistently evolves in our models under the influence of plate-driven mantle convection coupled with plume-induced buoyancy (Fig. 2). In the presence of a plume, the model with relative viscosity of the asthenosphere and craton as (1, 100), along with a strong temperature-dependent viscosity ($E = 10$), shows significant weakening of the craton base, which subsequently gets eroded by mantle flow (Figs. 3A–3D; Fig. S2 and Video S1 in the Supplemental Material[1]). Visible thinning

[1]Supplemental Material. Supplemental Figures S1–S5 and Videos S1–S4. Please visit https://doi.org/10.1130/GEOL.S.16985356 to access the supplemental material, and contact editing@geosociety.org with any questions.

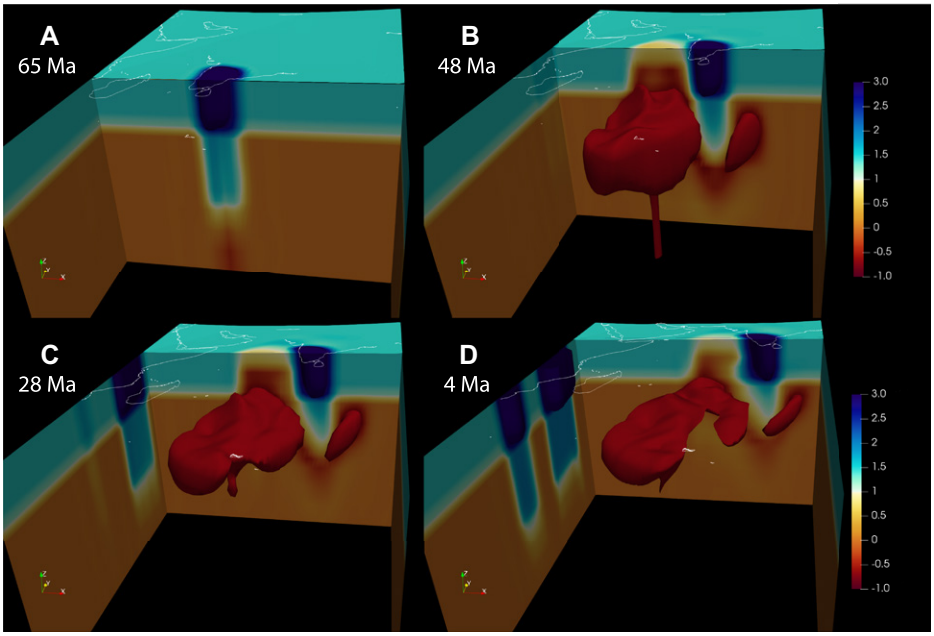


**Figure 3. Three-dimensional cross sections showing the thinning of the Indian craton in the presence of the Réunion plume. Section is 450 km deep and restricted within the coordinates of 30°E to 90°E and 60°S to 30°N. Colors represent the log of viscosity (visc) normalized against reference viscosity of $10^{21}$ Pa·s ($visc_0$). Cratons are marked by shades of blue, and the plume is indicated by shades of red. Relative (normalized) viscosity of the asthenosphere and craton is (1, 100) in this model, and $E = 10$ (where $E$ indicates strength of temperature dependence of viscosity; see text). At 48 Ma, the craton has already started thinning (B). In D, parts of the thick South African craton can be seen beside the thinned Indian craton. White borders indicate coastlines at the respective times.**

appears after ~15 m.y. (i.e., at ca. 50 Ma), and at least 60–70 km of root is found to have been destroyed by the present day (Fig. 3D; Fig. S2). The hot plume material is dragged by the Indian plate (Fig. 2) and makes the lithosphere-asthenosphere boundary (LAB) weaker. Approximately 50 km of thinning of the Indian non-cratonic lithosphere is observed in this model (Fig. S2; Video S1). When $E = 5$, root thickness gets reduced by ~10–20 km (Fig. S3; Video S2). For $E = 0$, there is no reduction of root, but slight vertical stretching of ~20 km is observed after 40 Ma (Fig. S4; Video S3). Similar vertical stretching is observed in the absence of a plume (Fig. S5; Video S4).

We calculated the areal deformation ($d$) of the Indian craton at each depth using the formula $d = 100 \times (A_t - A_o)/A_o$, where $A_o$ is the initial area of the Indian craton at 65 Ma at a particular depth, and $A_t$ is the area of the craton at any time $t$ at the same depth. If $d$ remains close to 0, it indicates that there is no net deformation of the craton. When $d$ reaches −100% at a particular depth, it indicates complete destruction of the craton at that depth. For example, if $d$ becomes −100% at 265 km depth at 50 Ma, it implies a reduction of 35 km of root thickness within the first 15 m.y. (Fig. S1). Thus we translated the horizontal areal deformation into vertical root reduction (Table S1).

In the absence of a plume, the areal deformation curves for the model with relative asthenosphere and craton viscosity of (1, 100) remain close to 0 at 265 and 240 km depths, indicating no root has been destroyed (Figs. 4A and 4B; Table S1). The craton root also remains intact for $E = 0$. An areal reduction of ~75% is observed at 265 km depth for the $E = 5$ model. For $E = 10$, −100% deformation occurs at 265 km and 240 km, indicating that at least 60 km of craton root has been destroyed; 35 km reduction takes place within the first 15 m.y., and 60 km thinning occurs after 35 m.y.

Models with the relative viscosity combination of asthenosphere and craton of (0.1, 100) (Figs. 4C–4F) show −100% areal deformation at 240 km depth, except in the case without a plume (Fig. 4D). In the presence of the plume, an initial 35 km of root reduction occurs within the first 7–8 m.y. (Fig. 4C). For $E = 0$, 60 km of root reduction takes place within 27 m.y. (Fig. 4D). With temperature-dependent viscosity ($E = 5$, 10), 60 km of reduction occurs within the first 12 m.y. For $E = 5$, ~110 km of root destruction happens within the first 42 m.y., and for $E = 10$, within the first ~20 m.y. Also, for $E = 10$, a total of ~130 km of root gets destroyed in 65 m.y. (Fig. 4F; Table S1). Cratons with viscosity 1000× that of their surroundings show at least 35 km of root destruction, regardless of asthenospheric strength, in the presence of strong temperature-dependent viscosity ($E = 10$) (Figs. 4G and 4H). However, this thinning takes place after 35–50 m.y.

## PLUME-INDUCED THERMOMECHANICAL EROSION OF THE CRATON

The major eruption of the Réunion plume resulted in the formation of the Deccan plateau (cf. Sharma et al., 2021), and its further magmatic activities are evident in the hotspot tracks in the Indian Ocean (Peters and Day, 2017). The plume eruption likely affected the dynamics of the Indian plate by inducing plate acceleration (Cande and Stegman, 2011) and continental breakup (Koptev et al., 2019) and by thinning the cratonic root under the plate (Kumar et al., 2007). In the presence of temperature-dependent viscosity, the plume weakens the base of the cratonic root. Due to plume-induced weakening, the cratonic root does not effectively stay "cratonic". Such a weaker root is thermomechanically eroded by the convective stresses exerted by mantle flow (Davies, 1994; Paul et al., 2019) and eventually gets assimilated into the surrounding asthenosphere. The intensity of weakening and mechanical erosion depends to some extent on the distance between the craton and the plume. If the plume is far away from the craton, thermomechanical erosion is mostly confined along the craton edge (Wang et al., 2015). In our models, the plume is just below the Indian craton, as it actually was at 65 Ma, resulting in extensive weakening of the craton interior. Moreover, because the Indian craton is smaller in size compared to other cratons (e.g., the South African craton), the effect of the plume-induced thermomechanical erosion is more profound.

Melting of a plume head could also potentially lead to recratonization (Liu et al., 2021). Our models do not produce melt generated from the Réunion plume. However, Bredow et al. (2017) showed that melt generation is insignificant below the thicker Indian lithosphere; instead, the melt has a tendency to migrate toward the thinner lithosphere away from the thick craton. Such deflection of plume-generated melt in the presence of a thick cratonic root has also been modeled under the Tanzanian craton (Koptev et al., 2015). Hence, the presence of melt is unlikely to significantly change the effect of thermomechanical erosion of the cratonic root.

## IMPLICATION FOR INDIAN PLATE VELOCITY

Thinning of the Indian craton due to plume-induced weakening did not happen instantaneously at 65 Ma. In our weakest viscosity combination case of (0.1, 100), the earliest 35 km root reduction took at least 5 m.y.; i.e., after 60 Ma (Fig. 4C). In other models, this reduction takes place much later. Kumar et al. (2007) proposed that the thinning of the Indian craton is a potential reason for the higher velocity of the Indian plate since ca. 65 Ma. Though we observe cratonic thinning in our models, the

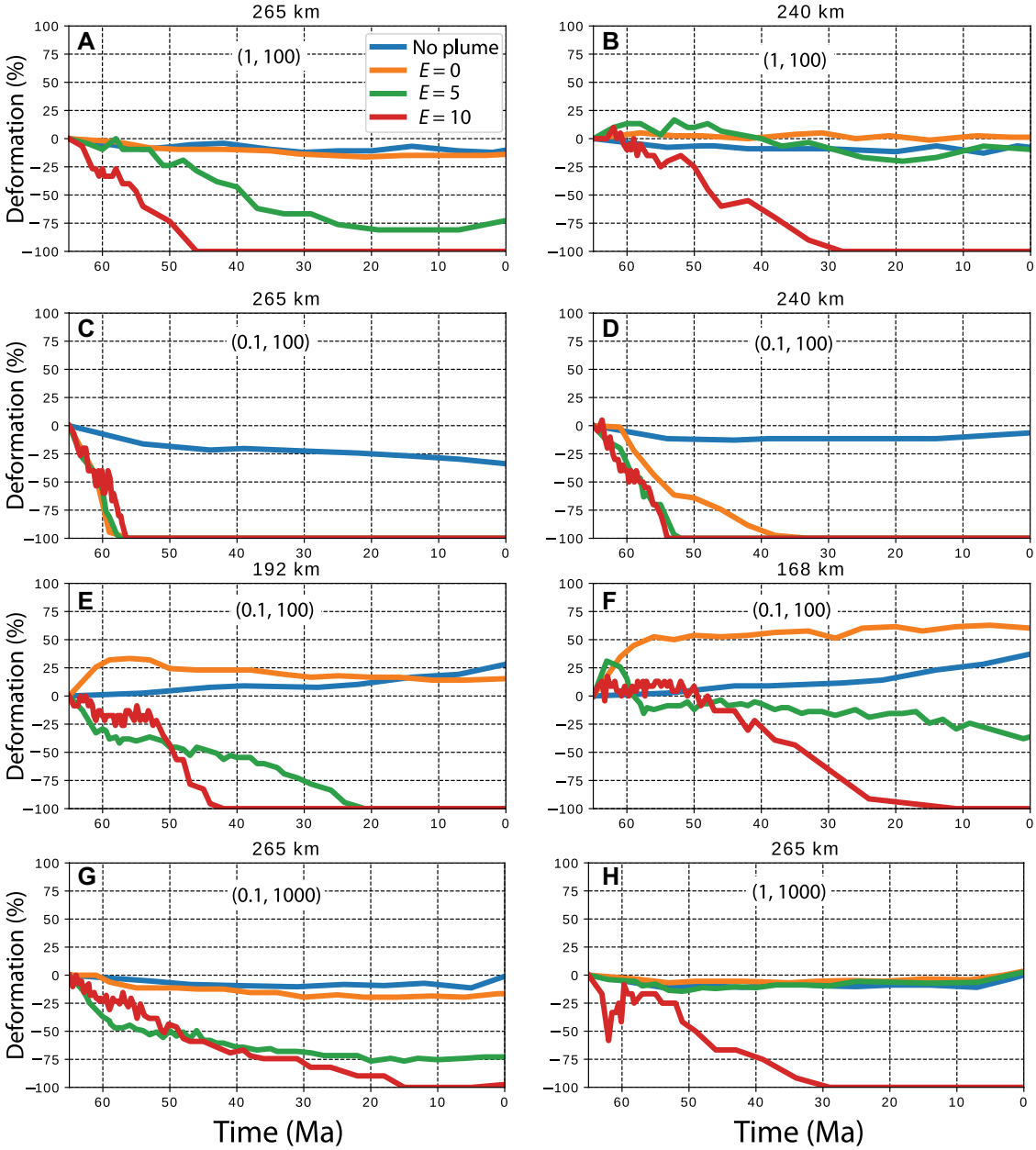


**Figure 4. Time-varying areal deformation curves at different depths from models of various viscosity combinations for the Indian craton. Viscosities are normalized to the reference viscosity of $10^{21}$ Pa·s. Deformation of –100% indicates complete destruction of the craton at the indicated depth. (A,B) Relative viscosity of asthenosphere and craton, respectively, of (1, 100). (C–F) Relative viscosity combination of (0.1, 100). (G) Relative viscosity combination of (0.1, 1000). (H) Relative viscosity combination of (1, 1000). Colored lines indicate cases with or without a mantle plume and temperature-dependent viscosity conditions, where *E* indicates strength of temperature dependence of viscosity (see text).**

cratonic root does not reduce to a significant extent when the peak velocity of the Indian plate is thought to have occurred (ca. 65–63 Ma; Pusok and Stegman, 2020). Pusok and Stegman (2020) also showed that the initial acceleration decayed by ca. 63–62 Ma and a second phase of higher velocity started at ca. 60 Ma that was sustained until ca. 52 Ma. They invoked a double subduction zone to explain the sustained higher velocity over ~10 m.y.

Thinning of the Indian craton could have contributed to the second phase of velocity increase, provided the craton is 100× more viscous compared to its surroundings and the asthenosphere viscosity is restricted to $10^{20}$ Pa·s (0.1, 100). Apart from this viscosity combination, the reduction of cratonic root takes place mostly after 50 Ma, implying that thinning of the craton may not have played a significant role in accelerating the Indian plate. Nevertheless, plume-induced weakening also reduces the non-cratonic lithosphere thickness by as much as ~50 km (Fig. S2), which might have played an important role in continental breakup (e.g., Koptev et al., 2019). Additionally, the hot plume material is dragged along with the Indian plate (Fig. 2), which could make the LAB 10×–100× weaker beneath the Indian plate. This weakening could effectively lubricate the LAB by reducing the frictional drag between the mantle and the overriding lithospheric plate (van Hinsbergen et al., 2011). The presence of a lubricated LAB could be a potential reason for the sustained higher velocity of the Indian plate until ca. 50–45 Ma.


## ACKNOWLEDGMENTS

CitcomS is maintained by Computational Infrastructure for Geodynamics (California, USA). Models were executed in the Cray XC40 system at the Supercomputer Education and Research Centre, Indian Institute of Science (Bangalore, India). The cost of the high-priority computational facility was supported by grant IE/REDA-20-1994 to A. Ghosh from the Indian Institute of Science–Institution of Eminence (IISc-IOE). J. Paul was partially funded by grant SP/DSTO-20-0014 from the Indian Department of Science and Technology (DST). We thank Giusy Lavecchia, Alexander Koptev, and an anonymous reviewer for their constructive reviews. Special thanks to Thorsten Becker for helping us with Visualization Tookit (https://vtk.org/) file conversion. Figures were made using Paraview 5.8.1, GPlates, and Generic Mapping Tools (versions 4 and 5).


## REFERENCES CITED


Artemieva, I.M., 2006, Global 1° × 1° thermal model TC1 for the continental lithosphere: Implications for lithosphere secular evolution: Tectonophysics, v. 416, p. 245–277, https://doi.org/10.1016/j.tecto.2005.11.022.

Boyden, J.A., Müller, R.D., Gurnis, M., Torsvik, T.H., Clark, J.A., Turner, M., Ivey-Law, H., Watson,

R.J., and Cannon, J.S., 2011, Next-generation plate-tectonic reconstructions using GPlates, *in* Keller, G.R., and Baru, C., eds., Geoinformatics: Cyberinfrastructure for the Solid Earth Sciences: Cambridge, UK, Cambridge University Press, p. 95–114, https://doi.org/10.1017/CBO9780511976308.008.

Bredow, E., Steinberger, B., Gassmöller, R., and Dannberg, J., 2017, How plume-ridge interaction shapes the crustal thickness pattern of the Reunion hotspot track: Geochemistry Geophysics Geosystems, v. 18, p. 2930–2948, https://doi.org/10.1002/2017GC006875.

Campbell, I.H., 2005, Large igneous provinces and the mantle plume hypothesis: Elements, v. 1, p. 265–269, https://doi.org/10.2113/gselements.1.5.265.

Cande, S.C., and Stegman, D.R., 2011, Indian and African plate motions driven by the push force of the Reunion plume head: Nature, v. 475, p. 47–52, https://doi.org/10.1038/nature10174.

Conrad, C.P., and Lithgow-Bertelloni, C., 2006, Influence of continental roots and asthenosphere on plate-mantle coupling: Geophysical Research Letters, v. 33, L05312, https://doi.org/10.1029/2005GL025621.

Cooper, C.M., Farrington, R.J., and Miller, M.S., 2020, On the destructive tendencies of cratons: Geology, v. 49, p. 195–200, https://doi.org/10.1130/G48111.1.

Davies, G.F., 1994, Thermomechanical erosion of the lithosphere by mantle plumes: Journal of Geophysical Research, v. 99, p. 15,709–15,722, https://doi.org/10.1029/94JB00119.

French, S.W., and Romanowicz, B., 2015, Broad plumes rooted at the base of the Earth's mantle beneath major hotspots: Nature, v. 525, p. 95–99, https://doi.org/10.1038/nature14876.

Ganguly, J., and Bhattacharya, P.K., 1987, Xenoliths in Proterozoic kimberlites from southern India: Petrology and geophysical implications, *in* Nixon, P.H., ed., Mantle Xenoliths: Chichester, UK, Wiley-Interscience, p. 249–265.

Koptev, A.I., and Ershov, A.V., 2011, Thermal thickness of the Earth's lithosphere: A numerical model: Moscow University Geology Bulletin, v. 66, p. 323–330, https://doi.org/10.3103/S014587521105005X.

Koptev, A., Calais, E., Burov, E., Leroy, S., and Gerya, T., 2015, Dual continental rift systems generated by plume-lithosphere interaction: Nature Geoscience, v. 8, p. 388–392, https://doi.org/10.1038/ngeo2401.

Koptev, A., Beniest, A., Gerya, T., Ehlers, T.A., Jolivet, L., and Leroy, S., 2019, Plume-induced breakup of a subducting plate: Microcontinent formation without cessation of the subduction process: Geophysical Research Letters, v. 46, p. 3663–3675, https://doi.org/10.1029/2018GL081295.

Kovács, I.J., et al., 2021, The 'pargasosphere' hypothesis: Looking at global plate tectonics from a new perspective: Global and Planetary Change, v. 204, 103547, https://doi.org/10.1016/j.gloplacha.2021.103547.

Kumar, P., Yuan, X., Kumar, M.R., Kind, R., Li, X., and Chadha, R.K., 2007, The rapid drift of the Indian tectonic plate: Nature, v. 449, p. 894–897, https://doi.org/10.1038/nature06214.

Lee, C.-T.A., Luffi, P., and Chin, E.J., 2011, Building and destroying continental mantle: Annual Review of Earth and Planetary Sciences, v. 39, p. 59–90, https://doi.org/10.1146/annurev-earth-040610-133505.

Lenardic, A., Moresi, L.-N., and Mühlhaus, H., 2003, Longevity and stability of cratonic lithosphere: Insights from numerical simulations of coupled mantle convection and continental tectonics: Journal of Geophysical Research, v. 108, 2303, https://doi.org/10.1029/2002JB001859.

Liu, J., Pearson, D.G., Wang, L.H., Mather, K.A., Kjarsgaard, B.A., Schaeffer, A.J., Irvine, G.J., Kopylova, M.G., and Armstrong, J.P., 2021, Plume-driven recratonization of deep continental lithospheric mantle: Nature, v. 592, p. 732–736, https://doi.org/10.1038/s41586-021-03395-5.

Mandal, P., 2017, Lithospheric thinning in the Eastern Indian Craton: Evidence for lithospheric delamination below the Archean Singhbhum Craton?: Tectonophysics, v. 698, p. 91–108, https://doi.org/10.1016/j.tecto.2017.01.009.

Matthews, K.J., Maloney, K.T., Zahirovic, S., Williams, S.E., Seton, M., and Müller, R.D., 2016, Global plate boundary evolution and kinematics since the late Paleozoic: Global and Planetary Change, v. 146, p. 226–250, https://doi.org/10.1016/j.gloplacha.2016.10.002.

Maurya, S., Montagner, J.-P., Kumar, M.R., Stutzmann, E., Kiselev, S., Burgos, G., Rao, N.P., and Srinagesh, D., 2016, Imaging the lithospheric structure beneath the Indian continent: Journal of Geophysical Research: Solid Earth, v. 121, p. 7450–7468, https://doi.org/10.1002/2016JB012948.

Naganjaneyulu, K., and Santosh, M., 2012, The nature and thickness of lithosphere beneath the Archean Dharwar Craton, southern India: A magnetotelluric model: Journal of Asian Earth Sciences, v. 49, p. 349–361, https://doi.org/10.1016/j.jseaes.2011.07.002.

Nataf, H.-C., and Ricard, Y., 1996, 3SMAC: An a priori tomographic model of the upper mantle based on geophysical modeling: Physics of the Earth and Planetary Interiors, v. 95, p. 101–122, https://doi.org/10.1016/0031-9201(95)03105-7.

Pandey, O.P., and Agrawal, P.K., 1999, Lithospheric mantle deformation beneath the Indian cratons: The Journal of Geology, v. 107, p. 683–692, https://doi.org/10.1086/314373.

Paul, J., and Ghosh, A., 2020, Evolution of cratons through the ages: A time-dependent study: Earth and Planetary Science Letters, v. 531, 115962, https://doi.org/10.1016/j.epsl.2019.115962.

Paul, J., Ghosh, A., and Conrad, C.P., 2019, Traction and strain rate at the base of the lithosphere: An insight into cratonic stability: Geophysical Journal International, v. 217, p. 1024–1033, https://doi.org/10.1093/gji/ggz079.

Peters, B.J., and Day, J.M.D., 2017, A geochemical link between plume head and tail volcanism: Geochemical Perspectives Letters, v. 5, p. 29–34, https://doi.org/10.7185/geochemlet.1742.

Pusok, A.E., and Stegman, D.R., 2020, The convergence history of India-Eurasia records multiple subduction dynamics processes: Science Advances, v. 6, eaaz8681, https://doi.org/10.1126/sciadv.aaz8681.

Sharma, J., Kumar, M.R., Roy, K.S., Pal, S.K., and Roy, P.N.S., 2021, Low-velocity zones and negative radial anisotropy beneath the plume perturbed northwestern Deccan volcanic province: Journal of Geophysical Research: Solid Earth, v. 126, e2020JB020295, https://doi.org/10.1029/2020JB020295.

Singh, A.P., Kumar, N., Rao, B.N., and Tiwari, V.M., 2021, Geopotential evidence of a missing lithospheric root beneath the eastern Indian shield: An integrated approach: Precambrian Research, v. 356, 106116, https://doi.org/10.1016/j.precamres.2021.106116.

Srinagesh, D., Rai, S.S., Ramesh, D.S., Gaur, V.K., and Rao, C.V.R., 1989, Evidence for thick continental roots beneath South Indian Shield: Geophysical Research Letters, v. 16, p. 1055–1058, https://doi.org/10.1029/GL016i009p01055.

van Hinsbergen, D.J.J., Steinberger, B., Doubrovine, P.V., and Gassmöller, R., 2011, Acceleration and deceleration of India-Asia convergence since the Cretaceous: Roles of mantle plumes and continental collision: Journal of Geophysical Research, v. 116, B0610, https://doi.org/10.1029/2010JB008051.

Wang, H., van Hunen, J., and Pearson, D.G., 2015, The thinning of subcontinental lithosphere: The roles of plume impact and metasomatic weakening: Geochemistry Geophysics Geosystems, v. 16, p. 1156–1171, https://doi.org/10.1002/2015GC005784.

Wang, Z., Kusky, T.M., Fu, J., Yuan, Y., and Zhu, P., 2016, Review of lithospheric destruction in the North China, North Atlantic, and Tanzanian cratons: The Journal of Geology, v. 124, p. 699–721, https://doi.org/10.1086/688608.

Zhong, S., Zuber, M.T., Moresi, L., and Gurnis, M., 2000, Role of temperature-dependent viscosity and surface plates in spherical shell models of mantle convection: Journal of Geophysical Research, v. 105, p. 11,063–11,082, https://doi.org/10.1029/2000JB900003.

Printed in USA